

Available online at www.sciencedirect.com

SciVerse ScienceDirect

journal homepage: www.elsevier.com/locate/he

Modeling of adsorbent based hydrogen storage systems

Bruce Hardy^{a,*}, Claudio Corgnale^a, Richard Chahine^b, Marc-André Richard^c,
Stephen Garrison^a, David Tamburello^a, Daniel Cossement^b, Donald Anton^a

^a Savannah River National Laboratory, Aiken, SC 29808, USA

^b Université du Québec à Trois-Rivières, Trois-Rivières, QC G9A 5H7, Canada

^c Institut de recherche d'Hydro-Québec, 600 de la Montagne, C.P. 990 Shawinigan, QC G9N 7N5, Canada

ARTICLE INFO

Article history:

Received 22 September 2011

Received in revised form

16 December 2011

Accepted 19 December 2011

Available online 23 January 2012

Keywords:

Adsorbent hydrogen storage

Adsorption hydrogen storage

MOF

Activated carbon

Adsorption hydrogen storage model

Modified Dubinin–Astakhov model

ABSTRACT

A numerical model was developed for the evaluation of adsorbent based hydrogen storage systems. The model utilizes commercial software and simultaneously solves the conservation equations for heat, mass and momentum together with the equations for the adsorbent thermodynamics. Conservation equations were derived for a general adsorbent bed-storage vessel configuration and the adsorbent thermodynamics were a modified form of the Dubinin–Astakhov model. The solver was the Comsol™ Multiphysics software. Real gas thermodynamic properties for hydrogen were used in the calculations. Model predictions were compared to data for charging an activated carbon based system. Applications of the model were made for charging of MOF-5™ and MaxSorb™ based systems that employ flow-through cooling as a means for controlling the adsorbent temperature during charging. In addition, the model was used to evaluate the contribution of pressure work to the total energy released during charging. It was found that flow-through cooling has the potential to be an effective means for heat removal and that the contribution of pressure work can be significant, depending on the type of adsorbent and the charging procedure. Copyright © 2012, Hydrogen Energy Publications, LLC. Published by Elsevier Ltd. All rights reserved.

1. Introduction

On board storage of hydrogen is a major technical obstacle for the development of practical hydrogen powered vehicles. While cryo-compression is a possible means for storage, and has been tested in prototype vehicles [1,2], a significant amount of energy is required to put hydrogen into either a liquefied or highly compressed cryogenic state. An alternative approach is to employ a medium that, by virtue of its chemical potential, stores a sufficient quantity of hydrogen at more moderate temperatures and pressures. Any such medium must uptake and retain the hydrogen in

a manner that readily allows its release. Storage media fall into 3 general classifications: chemical hydrides, which are recharged offboard the vehicle; adsorbents which uptake hydrogen via physisorption; and metal hydrides which undergo chemical reactions during the charging process and are refueled onboard the vehicle. All media based storage systems undergo complex, coupled physical processes during hydrogen uptake and discharge, making the use of numerical models essential for design and evaluation.

This paper focuses on adsorbents which show promise for meeting the DOE technical targets for storage system

* Corresponding author. Tel.: +1 803 646 4082.

E-mail address: bruce.hardy@srnl.doe.gov (B. Hardy).

Nomenclature	
c	Molar concentration of H_2 , mol/m ³
$C_{P\text{ Ads}}$	Specific heat of adsorbent, J/kg-K
$C_{P\text{ Bed}}$	Specific heat of non-adsorbing bed, J/kg-K
D_p	Effective mean pore diameter, m
E_a	Characteristic free energy of adsorption from the Dubinin–Astakhov model, J/mol $\equiv \alpha + \beta T$
\vec{g}	Gravitational acceleration vector, m/s ²
h	Molar enthalpy of the gas, J/mol
\underline{I}	2nd order identity tensor = δ_{ij}
k	Thermal conductivity, W/(m-K)
M_{Ads}	Molecular weight of adsorbent, kg/g-mol
M_{H_2}	Molecular weight of hydrogen, 0.002016 kg/g-mol
n_a	Absolute adsorption, (mol of H_2)/(kg of adsorbent)
n_{max}	Limiting adsorption, associated with the maximum hydrogen loading of the entire adsorption volume, (mol of H_2)/(kg of adsorbent)
n_{total}	Absolute adsorption, (mol of H_2)/(kg of adsorbent)
\hat{n}	Outward unit normal vector to surface element dS of volume V
P	Pressure, Pa
P_0	Pseudo-pressure for Dubinin–Astakhov model, or initial pressure, Pa
\vec{q}''	Heat flux vector, J/m ² -s
R	Gas constant = 8.314 J/(mol-K)
S	Surface area, m ²
S_0	Mass source of hydrogen per unit of total volume, kg/m ³ -s
T	Temperature, K
u	Molar internal energy of H_2 , J/mol
u_{Ads}	Specific internal energy of the adsorbent, J/kg
\tilde{u}_{Ads}	Molar internal energy of the adsorbent, J/mol
\tilde{u}_c	Molar internal energy of condensed phase (sorbed gas and adsorbent), J/mol
u_0	Molar internal energy of free gas at the system temperature T and a pressure of 1 atm, J/mol
U_a	Internal energy of the condensed phase of H_2 per mass of adsorbent, J/(kg of adsorbent)
\tilde{U}_a	Internal energy of the condensed phase of H_2 per mole of sorbed gas, J/(mol of sorbed gas)
V	Volume, m ³
V_a	Adsorbed volume per mass of adsorbent, m ³ /(kg of adsorbent). The void volume within the adsorbent for which the gas concentration exceeds that given by the equation of state, per mass of adsorbent.
V_v	Void volume per mass of adsorbent, m ³ /(kg of adsorbent). Measured by He filling.
v_i	i th component of the gas velocity vector, m/s
\vec{v}	Mean interstitial gas velocity vector, m/s or velocity of gas, m/s
\vec{v}_s	Superficial velocity vector, m/s
x_a	Mole fraction of adsorbed phase
x_{Ads}	Mole fraction of adsorbent
Z	Hydrogen compressibility factor
<i>Greek</i>	
α	Enthalpic contribution to the characteristic free energy of adsorption, E_a , J/mol
β	Entropic contribution to the characteristic free energy of adsorption, E_a , J/mol-K
ε	Effective porosity, volume available for flow = $\rho_{\text{Ads}}(V_v - V_a)$
δ_{ij}	Kronecker delta
ΔU_a	Internal energy of the condensed phase of the gas per mass of adsorbent at a temperature T and pressure P relative to free gas at a temperature T and a pressure of 1 atm, J/kg
ν	Molar volume of H_2 , m ³ /g-mol = 1/c
η_d	Dilatational viscosity of hydrogen, Pa-s = 0 Pa-s in this analysis
κ	Bed permeability, m ²
μ	Dynamic viscosity of hydrogen, Pa-s
ρ	Mass density of hydrogen, kg/m ³
ρ_{Ads}	Bulk mass density of adsorbent, kg/m ³
ρ_{Bed}	Bulk mass density of non-adsorbing bed, kg/m ³
$\underline{\tau}$	Fluid stress tensor, Pa

performance [3] over temperatures ranging from ~80–180 K. Although the numerical model developed for this study is applicable to a range of adsorbents, MaxSorb MSC-30™ (essentially the same as AX-21™) and MOF-5™ (Basolite Z100-H) are specifically addressed. The model employs governing equations which are described in detail in Section 3. Thermodynamic expressions for the quantity of hydrogen adsorbed and the internal energy of the adsorbed phase are based on the work of Richard, Bénard and Chahine [4,5]. Compressibility factor and property data for non-ideal hydrogen are obtained from the NIST REFPROP 23 database [6]. Model validation was performed against data from experiments with MaxSorb™ performed at the Université du Québec à Trois-Rivières (UQTR) as described in Richard et al. [7]. The model was applied to conceptual storage system configurations and a comparison between MaxSorb™ and MOF-5™ performance was made.

2. Background

V.S. Kumar et al. [8] developed a lumped model for a hydrogen storage vessel that used real hydrogen properties from the NIST web book and was applied to MOF-5™ by fitting a Langmuir isotherm to data for pressures from 1 to 30 bar and temperatures from 60 to 125 K. The model was similar to that of Richard, Bénard and Chahine [4,5], which was applied to MaxSorb™ via thermodynamics from modified Dubinin–Astakhov relations. The storage vessel evaluated in [8] used hydrogen flowing through the adsorbent bed as a coolant. Because the V.S. Kumar et al. model did not account for gradients in properties and hydrogen concentration; it was suitable for processes that do not transpire so rapidly that significant thermal gradients develop in the adsorbent.

V.S. Kumar and S. Kumar [9] derived 3-dimensional mass and energy conservation equations for an adsorbent storage vessel that were applied in 1-dimensional form. In the derivation of the governing equations, the relation between gas velocity and the pressure gradient was given by the Ergun equation, see Bird et al. [10]. However, the model in [9] was applied to an isobaric vessel, which implied an absence of pressure gradients. Hence, the gas velocity was derived from the mass balance and did not depend on flow resistance. The 1-dimensional system of equations, together with their boundary and initial conditions, were solved using the Comsol™ software. Hydrogen property data was obtained from the NIST web book and isotherm data for MOF-5™ was fit to a Langmuir-type isotherm. The model was used to evaluate the charging behavior of 3 different bed designs.

I. Gosh et al. [11] used 1-dimensional mass and energy conservation equations, together with an assumed linear velocity profile. Hydrogen was assumed to be an ideal gas and isotherms were given by a Langmuir fit to data for the form of activated carbon that was considered in the model. The model was compared to data obtained by Lamari et al. (2000) and was used to evaluate a conceptual storage vessel design.

Hermosilla-Lara et al. [12] and Momen et al. [13] employed isotherms based on the extended Dubinin–Astakhov equation described in Zhan, Li and Zhang [14]. Hydrogen was assumed to behave as an ideal gas in the 2-dimensional models, which employed the FLUENT™ software. Model predictions were compared to experiments performed at near-ambient temperatures, which were designed to measure transient temperature profiles during the charging of an activated carbon bed. Temperatures predicted by the models compared favorably with experimental measurements. Of particular interest, References [12] and [13] claimed that pressure work accounted for more than 70% of the energy released during the charging process, based on their model and experiments. However, it should be noted that at near-ambient temperatures the amount of hydrogen adsorbed is relatively small, resulting in a lower total heat release due to adsorption. Thus, for these conditions, one might intuitively expect pressure work to make a more significant contribution to the total thermal energy released during the charging process.

Paggiaro et al. [15] used the Comsol™ software to solve the conservation equations for a storage system based on activated carbon. The 2-dimensional axisymmetric model used real hydrogen properties, from the NIST 12 database. Excess adsorption isotherms were given by the Ono-Kondo model, and the Ergun equation was used in the momentum conservation equation. The particle diameter used in the Ergun equation, the bed thermal conductivity and a parameter for heat transfer from the adsorbent bed, were tuned to give a match between the model and experiments performed in this study. Among other things, the model was used to investigate the recirculation of hydrogen through the bed as a heat transfer mechanism, which was proposed in Schütz et al [16]. The model predicted that, because of the low thermal conductivity of the adsorbent bed, the use of flow-through cooling would result in much

shorter cooling times than could be obtained solely by conduction heat transfer to the walls of the storage vessel containing the adsorbent.

Xiao et al. [17] developed a model for an activated carbon storage system, which solved the conservation equations using the Fluent™ software. As for Paggiaro et al., the bed permeability was given by the Ergun equation. Isotherms were given by the modified Dubinin–Astakhov (DA) model discussed in M.-A. Richard et al. [4,5]. Hydrogen was assumed to be an ideal gas, and its specific heat and thermal conductivity, as well as the heat of adsorption were constant. The model was applied to the near-ambient temperature experiments performed by Hermosilla-Lara et al. [12] and the comparison of the Xiao et al. model with data was similar to that for the Hermosilla-Lara et al. model.

Vasilev and Kanonchik [18] applied the conservation equations in 2-dimensions, with ideal gas properties for hydrogen, to a hybrid adsorbent/metal-hydride storage medium. The rate of sorption in the medium was given by a kinetics expression that used adsorbent isotherms from the Dubinin–Radushkevich [4] equation. As part of the study, experiments were conducted for a configuration in which the medium was confined to an array of channels. Performance estimates for the storage system were obtained from the model.

3. Model description

The objective of this study was the development and application of a numerical model that had a sufficient level of detail for engineering evaluation of adsorbent based storage systems. It was desired to create a model capable of representing adsorption behavior for a range of vessel geometries, adsorbents and operating conditions, including operation at cryogenic temperatures and high pressures. The model developed in this study distinguishes itself from those discussed in the literature review, in that it employs the following combination of features:

1. Systematically derived mass momentum and energy conservation equations for an adsorbent based storage system.
2. Formulation of the governing equations to describe gas flow from an open channel into the packed adsorbent bed.
3. Inclusion of terms for viscous dissipation and pressure work.
4. The ability to account for energy transport in vessel structures and heat transfer elements.
5. The use of real hydrogen properties; those from the NIST REFPROP23 database [6] were used.
6. The use of temperature dependent specific heats for the adsorbent bed; those used were based on Pyda et al. [19] and are suitable for cryogenic temperatures.
7. Adsorbent thermodynamics and isotherms are based on the Dubinin–Astakhov DA equations having the form in [5].
8. Modular construction of the numerical model which readily permits replacement of the DA thermodynamic model with others.

9. Adaptability of the model to represent single gas species other than hydrogen, if the parameters for the DA thermodynamic model are available.

The model was applied to activated carbon, MaxSorb™ (MSC-30) and to MOF-5™ (Basolite™ Z100-H). Application to other adsorbent media is relatively straightforward via modification of the parameters of the DA equations and other material properties.

3.1. Governing equations

Governing equations for the adsorbent model are based on the conservation of mass, momentum and energy.

3.1.1. Conservation of mass

The integral form of the mass conservation equation is

$$\frac{\partial}{\partial t} \int_V \varepsilon \rho dV = - \int_S \rho \vec{v} \cdot \hat{n} \varepsilon dS + \int_V S_0 dV \quad (1)$$

For fixed ε the differential form of the mass conservation equation becomes

$$\varepsilon \frac{\partial \rho}{\partial t} = -\varepsilon \nabla \cdot (\rho \vec{v}) + S_0 \quad (2)$$

Within a packed bed of adsorbent, the volumetric mass source term, S_0 , is

$$S_0 = -M_{H_2} \rho_{Ads} \frac{\partial n_a}{\partial t} \quad (3)$$

In a porous media outside the adsorbent bed $S_0 = 0$ and Eq. (4) becomes

$$\varepsilon \frac{\partial \rho}{\partial t} + \nabla \cdot (\rho \vec{v}_s) = 0 \quad (5)$$

For flow in the absence of a porous media, ε , is 1, $\vec{v}_s = \vec{v}$, and the conservation of mass equation is

$$\frac{\partial \rho}{\partial t} + \nabla \cdot (\rho \vec{v}) = 0 \quad (6)$$

Eq. (6) applies to open channels within the storage vessel or connecting tubing. Note that the superficial velocity, \vec{v}_s , of hydrogen is used for porous media, while the velocity, \vec{v} , is used in open channels.

3.1.2. Conservation of momentum

For flow in an open channel the momentum conservation equation has the usual form

$$\rho \frac{\partial \vec{v}}{\partial t} + \rho (\vec{v} \cdot \nabla \vec{v}) = -\nabla P + \nabla \cdot \left[\mu (\nabla \vec{v} + \nabla \vec{v}^T) \right] - \nabla \cdot \left[\left(\frac{2\mu}{3} - \eta_d \right) \left(\frac{1}{\varepsilon} \right) (\nabla \cdot \vec{v}) \underline{\underline{I}} \right] + \rho \vec{g} \quad (7)$$

The momentum conservation equation in the adsorbent bed is first expressed in integral form to ensure that all contributions are included

$$\underbrace{\frac{\partial}{\partial t} \int_V [\varepsilon \rho \vec{v}] dV}_{\text{Rate of change in gas momentum in void space}} = \underbrace{- \int_S [P \hat{n} \varepsilon] dS}_{\text{Rate of momentum transfer due to pressure force on surface of control volume}} - \underbrace{\int_S [(\hat{n} \cdot \underline{\underline{\tau}}) \varepsilon] dS}_{\text{Rate of momentum transfer due to viscous force on surface of control volume}} - \underbrace{\int_S [\vec{v} (\varepsilon \rho (\vec{v} \cdot \hat{n}))] dS}_{\text{Net outflow of momentum due to convection out of control volume}} - \underbrace{\int_V \left[\varepsilon \frac{\mu}{\kappa} \vec{v}_s \right] dV}_{\text{Momentum source due to packed bed}} + \underbrace{\int_V [\varepsilon \rho \vec{g}] dV}_{\text{Momentum source due to gravity}} \quad (8)$$

The absolute adsorption of hydrogen, n_a , is obtained from isotherms based on the modified DA model. By using an isotherm to describe hydrogen uptake, it is tacitly assumed that there is negligible mass transfer resistance between the bulk gas and the adsorbent sites, and that adsorption kinetics are very rapid. It may, however, be necessary to reconsider the assumption of rapid mass transfer for adsorbents that have been compacted or those that incorporate an additive such as a binder or an amendment to enhance thermal conductivity.

Substituting Eq. (3) into Eq. (2) gives the mass conservation equation in the adsorbent bed

$$\varepsilon \frac{\partial \rho}{\partial t} + \nabla \cdot (\rho \vec{v}_s) = -M_{H_2} \rho_{Ads} \frac{\partial n_a}{\partial t} \quad (4)$$

where: $\vec{v}_s = \varepsilon \vec{v}$ = the superficial gas velocity.

After some manipulation, Eq. (7) takes the form

$$\frac{\rho}{\varepsilon} \frac{\partial \vec{v}_s}{\partial t} + \left(\frac{\mu}{\kappa} + \frac{S_0}{\varepsilon^2} \right) \vec{v}_s = -\nabla P + \nabla \cdot \left[\frac{\mu}{\varepsilon} (\nabla \vec{v}_s + \nabla \vec{v}_s^T) \right] - \nabla \cdot \left[\left(\frac{2\mu}{3} - \eta_d \right) \left(\frac{1}{\varepsilon} \right) (\nabla \cdot \vec{v}_s) \underline{\underline{I}} \right] \quad (9)$$

In the packed bed, the term representing the gravitational force, $\rho \vec{g}$, makes an insignificant contribution to the momentum balance. Further, inertial term, $\rho/\varepsilon^2 (\vec{v}_s \cdot \nabla \vec{v}_s)$, is negligible relative to flow resistance by the packed bed. Thus, the inertial and gravitational terms were neglected in Eq. (9).

In a packed bed the permeability, κ , in Eqs. (8) and (9) may be represented by the Ergun equation, Bird et al. [10].

$$\frac{1}{\kappa} = \underbrace{150 \frac{(1-\varepsilon)^2}{D_p^2 \varepsilon^3}}_{\text{Contribution of viscous effects}} + \underbrace{1.75 \frac{\rho}{\mu D_p} \frac{(1-\varepsilon)}{\varepsilon^3} |\vec{v}_s|}_{\text{Contribution of inertial effects}} \quad \text{inverse of Ergun permeability} \quad (10)$$

The Ergun permeability was chosen for this model as it applies over a wide range of bed Reynolds numbers, $D_p \rho |\vec{v}_s| / \mu (1 - \varepsilon)$, and applies to superficial velocities at which viscous dissipation may make a significant contribution to the heat source.

It should be remarked that the momentum conservation equation for packed beds in Comsol™ v3.5a uses the term S_0 in place of S_0/ε^2 , which while not consistent with a rigorous derivation, was found to have an insignificant effect on the calculated pressure and velocity components of within the adsorbent media for the conditions evaluated in this study. This is again due to the dominance of the contribution of momentum source for the packed bed.

In an open channel, without porous media, the momentum conservation equation is

$$\rho \frac{D\vec{v}}{Dt} = -\nabla P - \nabla \cdot \underline{\underline{\tau}} + \rho \vec{g} \quad (11)$$

where: \vec{v} = Velocity of hydrogen (m/s).

The equation for momentum conservation in a packed bed without hydrogen sources or sinks is obtained from Eq. (9) by setting the mass source term, S_0 , to zero.

3.1.3. Conservation of energy

For an open channel, the equation for energy conservation has the well-known form

$$c \frac{\partial h}{\partial T} \frac{\partial T}{\partial t} - \nabla \cdot k \nabla T = -c \frac{\partial h}{\partial T} \vec{v} \cdot \nabla T - \frac{T}{c} \frac{\partial c}{\partial T} \left(\frac{\partial P}{\partial t} + \vec{v} \cdot \nabla P \right) - \underline{\underline{\tau}} : \nabla \vec{v} \quad (12)$$

Energy conservation in the adsorbent bed is first expressed in integral form to ensure that all contributions are included

It is assumed that the condensed phase, consisting of the adsorbent and sorbed phase, comprise an ideal mixture, which by definition means that the thermodynamic properties of the adsorbent are not affected by the sorbed gas. The internal energy of the condensed phase is thus,

$$\tilde{u}_c = x_a \tilde{U}_a + x_{Ads} \tilde{u}_{Ads}$$

where \tilde{u}_c , \tilde{U}_a and \tilde{u}_{Ads} are molar quantities.

Since the enthalpy and internal energy of the adsorbent is essentially independent of pressure,

$$\frac{\partial u_{Ads}}{\partial t} \approx \frac{du_{Ads}}{dT} \frac{\partial T}{\partial t} = C_{P Ads} \frac{\partial T}{\partial t}$$

Eq. (13) can be put into the form

$$\begin{aligned} & \varepsilon c \frac{\partial h}{\partial T} \frac{\partial T}{\partial t} - \nabla \cdot k \nabla T \\ &= -c \frac{\partial h}{\partial T} \vec{v}_s \cdot \nabla T - \underbrace{\frac{T}{c} \frac{\partial c}{\partial T} \left(\varepsilon \frac{\partial P}{\partial t} + \vec{v}_s \cdot \nabla P \right)}_{\text{Pressure work}} \\ &+ \underbrace{\frac{\mu}{\varepsilon} \left[(\nabla \vec{v}_s + \nabla^T \vec{v}_s) - \left(\frac{2}{3} - \eta_d \right) \nabla \cdot \vec{v}_s \underline{\underline{I}} \right] : \nabla \vec{v}_s}_{\text{Viscous dissipation}} \\ &- \frac{h S_0}{M_{H_2}} - \rho_{Ads} \left(\underbrace{\frac{\partial \Delta U_a}{\partial t} + \frac{\partial (u_0 n_a)}{\partial t}}_{\text{Sorption Energy}} + C_{P Ads} \frac{\partial T}{\partial t} \right) \end{aligned} \quad (14)$$

where the contribution of kinetic energy, $S_0(\vec{v}_s \cdot \vec{v}_s)/2\varepsilon^2$, has been neglected.

In Eq. (14), the term

$$\begin{aligned} & \frac{\partial}{\partial t} \int_V \left[\underbrace{\varepsilon c u}_{\text{Internal energy of hydrogen in pores}} + \underbrace{\varepsilon \rho \left(\frac{\vec{v} \cdot \vec{v}}{2} \right)}_{\text{Kinetic energy of hydrogen in pores}} + \rho_{Ads} \left(\underbrace{U_a}_{\text{Internal energy of sorbed phase per mass of adsorbent}} + \underbrace{u_{Ads}}_{\text{Specific internal energy of adsorbent}} \right) \right] dV \\ &= \underbrace{- \int_S \left[\left(h + M_{H_2} \left(\frac{\vec{v} \cdot \vec{v}}{2} \right) \right) c \vec{v} \cdot \hat{n} \varepsilon \right] dS}_{\text{Net rate of enthalpy convected into the control volume}} - \underbrace{\int_S [(\hat{n} \cdot \underline{\underline{\tau}}) \cdot \vec{v}] \varepsilon dS}_{\text{Work done by viscous forces due to fluid only}} \\ & \quad - \underbrace{\int_S [\vec{q}'' \cdot \hat{n}] dS}_{\text{Net rate of heat flow into the control volume}} + \underbrace{\int_V [\rho (\vec{v} \cdot \vec{g}) \varepsilon] dV}_{\text{Rate of work done by gravitational force (negative rate of potential energy increase)}} - \underbrace{\int_V \left[\frac{\mu}{\varepsilon} (\vec{v}_s \cdot \vec{v}) \varepsilon \right] dV}_{\text{Work done by viscous forces due to the presence of the bed}} \end{aligned} \quad (13)$$

$$\frac{\partial \Delta U_a}{\partial t} + \frac{\partial (u_0 n_a)}{\partial t}$$

represents the rate of change of internal energy of the sorbed phase (hydrogen), where ΔU_a is obtained from the modified DA model [4,5].

For rapid pressurization, the pressure work term of Eq. (14) (specifically the part associated with $\partial P/\partial t$) will contribute significantly to the thermal energy dissipated within the storage vessel. The location at which the temperature rise associated with pressure work is most significant depends on the vessel configuration and does not necessarily occur in the adsorbent bed.

The equation for energy conservation in a packed bed without hydrogen sources or sinks is obtained from Eq. (14) by setting the terms, S_0 and $(\partial \Delta U_a/\partial t) + (\partial (u_0 n_a)/\partial t)$ to zero and replacing $\rho_{Ads} C_{P, Ads}$ with $\rho_{Bed} C_{P, Bed}$.

3.2. Hydrogen properties

Properties for real hydrogen, as functions of temperature and pressure, are obtained from the NIST REFPROP 23 v8.0 database [6]. To allow taking derivatives in Comsol™ and to increase the speed of computations, the property data is expressed in terms of regressions. For all regressions T is in K and P is in Pa. The regressions were fit for temperatures ranging from 70 K to 450 K and pressures ranging from 0.050 MPa to 35 Mpa. Comparisons with parameter values from the NIST database indicate accuracy within 0.58% for the enthalpy and 0.63% for the compressibility factor.

The hydrogen compressibility factor is expressed as

$$Z(T, P) = 1 + A_z(T) * P + B_z(T) * P^2 + C_z(T) * P^3 + D_z(T) * P^4$$

The molar hydrogen enthalpy (J/mol) is expressed as

$$h(T, P) = A_h(P) * T + B_h(P) + \frac{C_h(P)}{T} + \frac{D_h(P)}{T^2}$$

The hydrogen thermal conductivity (W/m-K) is expressed as

$$k(T, P) = A_k(P) + B_k(P) * T + C_k(P) * T^2 + D_k(P) * T^3 + E_k(P) * T^4 + F_k(P) * T^5$$

The hydrogen viscosity (Pa-s) is expressed as

$$\mu(T, P) = A_\mu(P) + B_\mu(P) * T + C_\mu(P) * T^2 + D_\mu(P) * T^3 + E_\mu(P) * T^4 + F_\mu(P) * T^5$$

The coefficients in the above expressions are obtained from spline fits to tabulated values as functions of T or P , respectively.

3.3. Adsorbent properties

3.3.1. Adsorbent specific heat

The specific heat for carbon was obtained from Pyda et al. [19]; where it is expressed as a complicated function of temperature. To increase computational speed, values of the carbon specific heat obtained from the Pyda expression were tabulated with their corresponding temperatures, input to Comsol™ and interpolated using a cubic spline. Due a lack of data, the temperature dependent specific heat of MOF-5™ was

estimated by scaling the correlation of [19] to the known specific heat of MOF-5™ at temperatures between 25 and 65 °C, and applying the scale factor for the entire temperature range.

3.3.2. Thermodynamic adsorbent models

Isotherms and the sorbed phase internal energy are obtained from the modified DA model [4,5]. The model requires 5 parameters: n_{max} , α , β , P_0 , and V_a . The first four parameters: n_{max} , α , β and P_0 are directly from the model for absolute adsorption. The last parameter, V_a , represents the volume of the adsorbed hydrogen and is used to convert excess adsorption experimental data to the absolute adsorption described by the model. These parameters were obtained by fitting the DA model to excess adsorption data for a gas-adsorbent combination and are listed in Table 1.

From Reference [5] the absolute adsorption, n_a , is

$$n_a = n_{max} \exp \left[- \left(\frac{RT}{E_a} \right)^2 \ln^2 \left(\frac{P_0}{P} \right) \right] \quad (15)$$

where: $E_a = \alpha + \beta T$

The total moles of hydrogen per mole of adsorbent, n_{total} , is defined as

$$n_{total} = n_a + \rho_g (V_v - V_a) \quad (16)$$

n_{total} represents the total amount of gas, per mass of adsorbent, stored by adsorption in the adsorbed volume, V_a , and by compression within the void volume, V_v , of the adsorbent.

The effective porosity for the adsorbent bed is

$$\varepsilon \equiv \rho_{Ads} (V_v - V_a) \quad (17)$$

From References [4] and [5], the internal energy of the condensed phase, U_a , is

$$U_a \equiv \Delta U_a + u_0 n_a \quad (18)$$

where ΔU_a is expressed as

$$\Delta U_a = - \frac{n_{max} \alpha \sqrt{\pi}}{2} \left[1 - \operatorname{erf} \left(\sqrt{-\ln \left(\frac{n_a}{n_{max}} \right)} \right) \right] + n_a \left[RT - \alpha \sqrt{-\ln \left(\frac{n_a}{n_{max}} \right)} \right] \quad (19)$$

Table 1 – Parameters for the modified Dubinin–Astakhov equations.

Parameter	MaxSorb™ ^a	MOF-5™ ^b
n_{max} [mol/kg of adsorbent]	71.6	88.1
P_0 [MPa]	1470	322
α [J/mol]	3080	2403
β [J/mol-K]	18.9	11.5
V_a [m ³ /(kg of adsorbent)]	0.00143	0.00194
V_v [m ³ /(kg of adsorbent)]	0.0029	0.0062

^a MaxSorb parameters are given in [4 and 5].

^b MOF-5™ parameters were provided by the Ford Motor Company as preliminary-release data.

Table 2 – Heat and mass transfer parameters.

Parameter	Value for Hydrogen Adsorption	References
MaxSorb bulk density	300 kg/m ³	[4]
MOF-5™ bulk density	150 kg/m ³	Data from Ford
Carbon (MaxSorb) specific heat	Correlation	[19]
MOF-5™ specific heat	Carbon (MaxSorb) specific heat correlation scaled by a factor of 1.0085	Scaled, based on Ford estimate
Bed thermal conductivity	0.2 W/m-K for MaxSorb 0.3 W/m-K for MOF-5™	[21] [22]
Mean pore diameter for MaxSorb and MOF-5™	73 μm	Assumed
Hydrogen density, thermal conductivity, enthalpy and viscosity	Correlations	[6]

3.3.3. Heat and mass transfer parameters for adsorbents

Although the parameters governing the thermodynamic models for MaxSorb™ and MOF-5™ are available, the same does not hold for parameters that characterize heat and mass transfer in the adsorbent bed. Table 2 contains estimated values of heat and mass transfer parameters for the bulk adsorbents.

3.4. Software

The system of governing equations, together with boundary conditions and ancillary equations are solved using the Comsol™ v3.5a finite element software [20].

4. Results

4.1. Comparison with data

The model was compared to experiments performed at UQTR in which MaxSorb™ was charged with hydrogen, as discussed in Reference [7]. The apparatus used in these experiments was originally designed to evaluate the global thermal behavior of the adsorbent system during the charging process. Application to the detailed model of this paper required the approximation of boundary conditions to properly account for parasitic and other forms of heat transfer.

4.1.1. Model geometry

Reference [7] gives a detailed description of the apparatus used for the UQTR experiments, which is shown schematically in Fig. 1. As shown in Figs. 1 and 2 the storage vessel was contained in a Dewar. The dimensions of the storage vessel, which contained the adsorbent, are shown in Fig. 2. The total internal volume of the storage vessel was 2.5 L; the mass of MaxSorb™ contained in the vessel was 0.671 kg. Charging tests were performed at low temperatures, whereupon the Dewar was filled with liquid nitrogen. Temperatures, flowrates and pressures within the storage vessel were measured during the charging process. The model of the storage vessel was axisymmetric and employed boundary conditions at the vessel surface. Materials comprising the vessel, its contents, the thermocouple support and the thermocouple locations, along with applied boundary conditions, are shown in Fig. 3.

4.1.2. Data comparison

For the tests, the initial vessel pressure was 1.82 bar and the initial bed and vessel temperatures were approximately 79 K. Hydrogen was fed to the vessel at approximately 16 SLPM at a temperature ranging from 290 to 296 K, over the

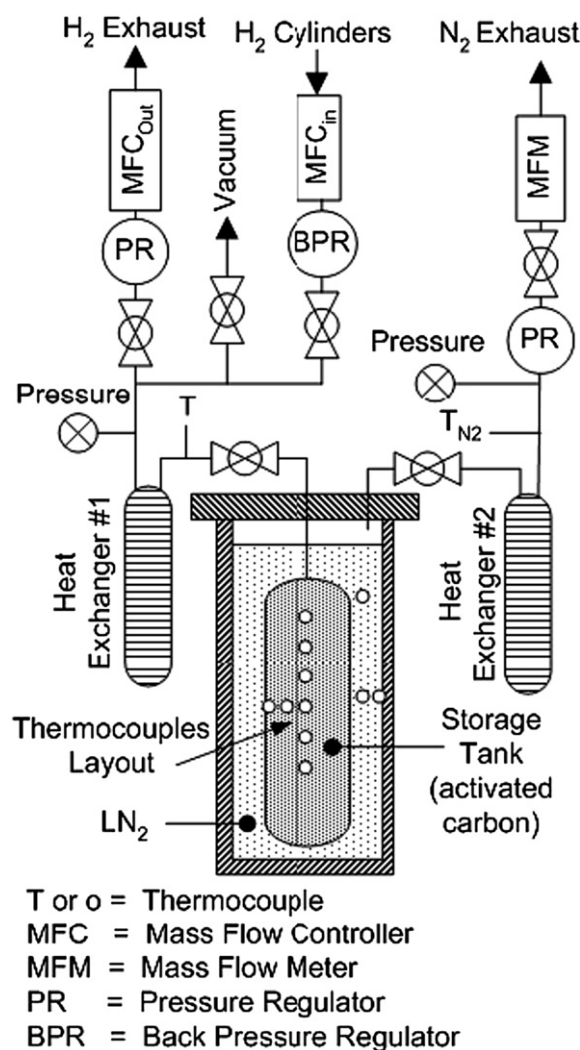


Fig. 1 – Schematic of UQTR experimental apparatus. As shown, the experiment is set up for low temperature tests. Liquid nitrogen is replaced with water or air for the high temperature tests.

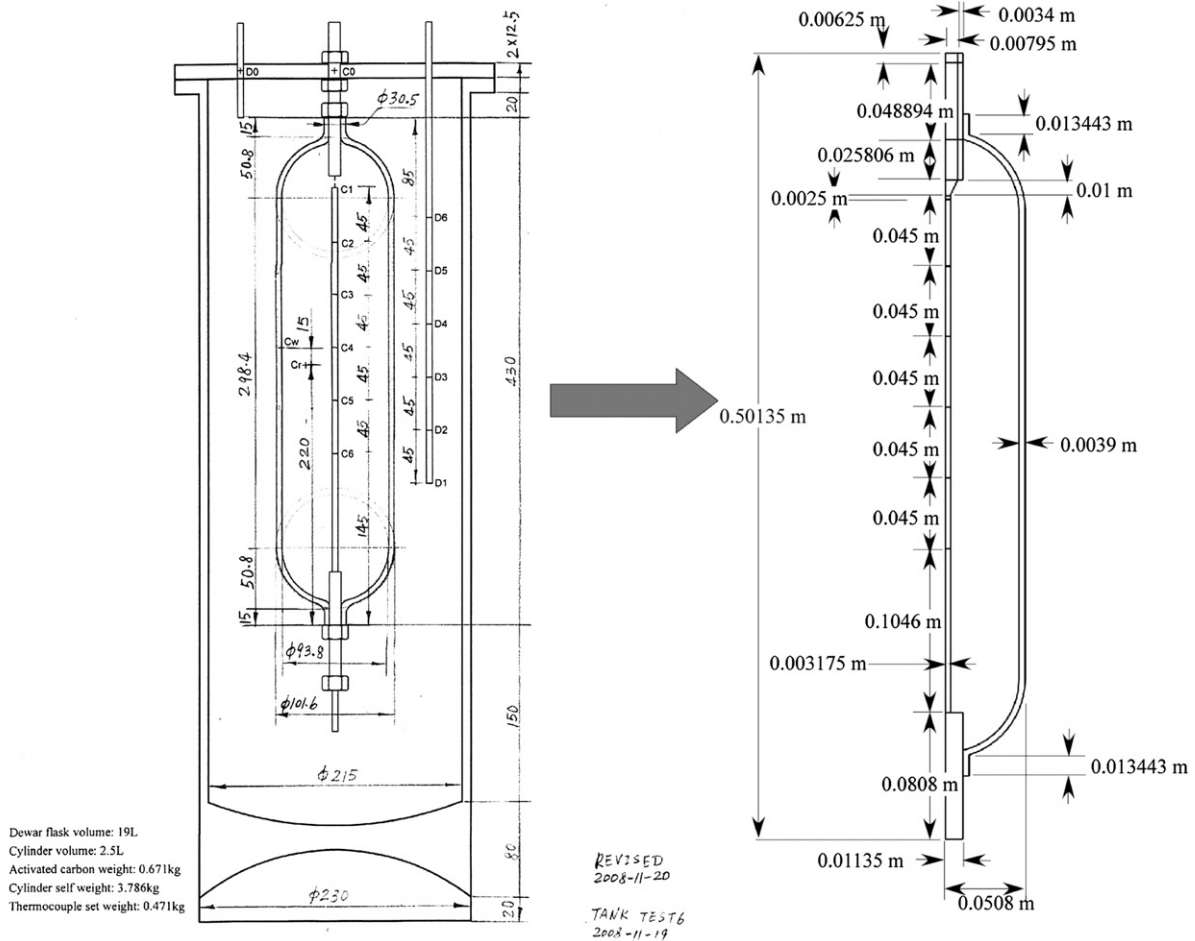


Fig. 2 – Rendering of UQTR experimental apparatus (left) as numerical model (right). Dimensions used in the model are shown in figure on the right. The total volume of the storage vessel was 2.5 L and contained 0.671 kg of MaxSorb™.

approximately 1600 s duration of the charging transient. The inlet flow boundary condition for the model was the measured transient inlet pressure. The boundary conditions applied at the surface of the vessel were: the measured liquid nitrogen temperature of approximately 80 K for Region 1 in Fig. 3, while an adiabatic boundary condition was applied for Region 2.

Fig. 4 shows the measured and predicted temperatures for the axial thermocouples, TC1, TC2, TC3 and TC6. Because the temperatures for thermocouples TC4, TC5 and TC6 were very close, the temperature profiles for thermocouples TC4 and TC5 were omitted to clarify the graph. The greatest difference between predicted and measured temperatures occurred for TC2. Differences between predicted and measured temperatures tended to decrease for TC3 through TC6. Overall differences between temperatures from the model and data are similar to those in Reference [15], which also compared a model and data for cryogenic hydrogen adsorption on activated carbon.

Major contributors to the observed differences include:

1. Boundary conditions on the vessel.

- a. The model was found to be very sensitive to boundary conditions applied to the wall of the tank that

contained the adsorbent; this pertains to both a temperature and/or a heat flux boundary condition.

- b. In the experiments, nitrogen was added to the Dewar before charging and boiled off without replacement during the charging process [7]. Therefore, the location of the interface between gaseous and liquid nitrogen changed during the charging transient, moving downward along the wall of the storage vessel. The moving interface, together with boiling heat transfer and convection resulted in a very complex thermal boundary condition at the surface of the storage vessel. Convection heat transfer from the storage vessel to the liquid and gas phase nitrogen occupying the Dewar was extremely difficult to characterize; correlations for this type of convection heat transfer are not available.

2. Variation in the bulk bed density. The density of the MaxSorb™ likely varied within the vessel. This would affect local heat generation rates, volumetric heat capacity (ρC_p), thermal contact resistance and bed thermal conductivity. Also, if the bed density were reduced above and along the thermocouple assembly, it would enhance the transport of hot gas fed to the vessel; especially along

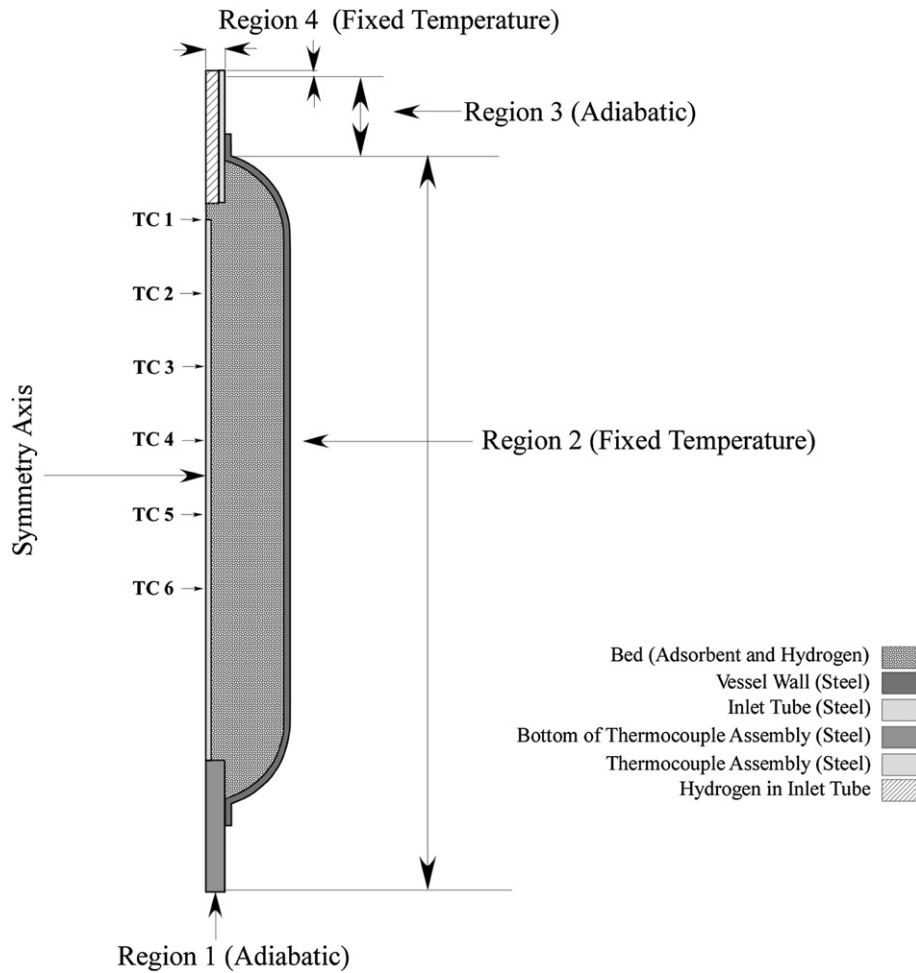


Fig. 3 – Material composition and boundary conditions used in model.

the upper part of the thermocouple. If this occurred, it would explain the rapid initial temperature rise observed for TC1 and TC2; indeed, scoping calculations showed that this could occur.

3. Parasitic heat transfer through the metal thermocouple support. It was known; see Reference [7], that heat leaks to the ambient existed. While the amount of heat leakage established in Ref. [7] suffices for a global energy balance,

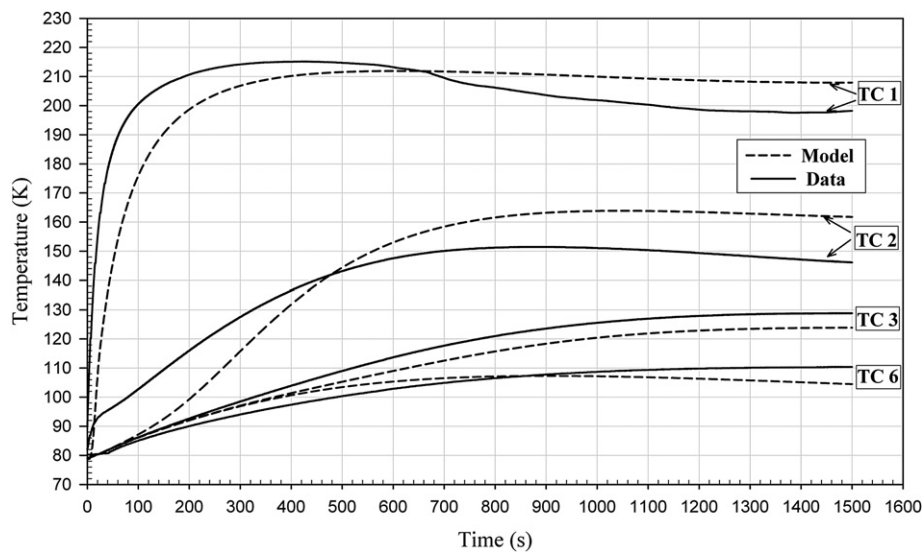


Fig. 4 – Validation of model against low temperature data.

more precise information is required for the detailed model.

4. Scoping calculations have shown that, as expected, the model is quite sensitive to changes in the adsorbent thermal conductivity. In the validation models, the thermal conductivity of the adsorbent was given an approximate fixed value of 0.2 W/m-K. It is known, however, that the adsorbent thermal conductivity decreases with decreasing temperature. Temperature gradients within the bed will therefore yield non-uniform bed thermal conductivities, which will impact heat transfer.

Total hydrogen concentrations calculated by the model are shown in Fig. 5. Although the model had the ability to compute spatial pressure gradients within the vessel, it was found that the pressure was nearly uniform during the charging process. At 100 s, the model predicted that the hydrogen concentration was lowest at the top of the adsorbent bed. This was due to the influx of gas at a temperature of approximately 290 K, which reduced the amount of adsorbed hydrogen at that location. As the transient progressed, the total amount of stored hydrogen increased. However, the heat released during the charging process resulted in elevated temperatures, and relatively lower amounts of stored hydrogen, in the interior of the bed. Higher hydrogen concentrations were predicted along the cold surfaces in the vessel, which included the tank wall and the central thermocouple support. Lower temperatures occurred at the surface of the steel thermocouple support because it provided a path for heat transfer to the liquid nitrogen within the Dewar.

4.2. Application

4.2.1. Storage vessel charging

The low thermal conductivity of MaxSorb™ and MOF-5™ makes it difficult to employ conduction to remove heat

released during the charging process. Enhancement of the adsorbent thermal conductivity would either require amendments, such as expanded natural graphite, or close spacing of heat transfer surfaces to reduce the conduction transport length. Either way, the gravimetric and volumetric capacities of the bed would be compromised by the addition of non-adsorbing material. An alternative method for heat removal is passing cold hydrogen through the bed to transfer heat by convection [8,15,16]. For this process, some hydrogen would be adsorbed and the remainder would be cycled through the bed and recovered, see Figs. 6–8. Because adequate hydrogen superficial velocity is required for flow-through cooling to be viable, the bed permeability must be high enough that the required flow can be attained for reasonable pressure gradients.

According to the 2017 DOE Technical Targets [3], a storage vessel must be charged with 5 kg of available hydrogen in 3.3 min. The total amount of hydrogen available is that recovered by transitioning the storage vessel from its initial state at full charge to its final, “empty,” state upon return to the fueling station. The 5 kg quantity is interpreted as the amount of hydrogen available to supply power to propel the vehicle. Integrated system models indicate that an additional 0.6 kg of hydrogen must be stored to power storage system support components, such as pumps, heaters, etc. Therefore, a total of 5.6 kg of hydrogen must be stored in 3.3 min. The integrated system model, which employed a global energy balance for the vessel and assumed a “nominal” rate of heat removal, was used to estimate the volume of the storage vessel, shown in Figs. 6–8. For this reason, the total capacity of the vessel exceeds 5.6 kg of available hydrogen and, for more rapid charging times, the vessel stores more than 5.6 kg of available hydrogen. Both adsorbed and compressed gas phase hydrogen stored in the void volume of the adsorbent are included in the total. The adsorbents, MaxSorb™ and MOF-5™, were assumed to be in nominal powder form and occupied a volume of 0.164 m³. Prior to charging the storage vessel was

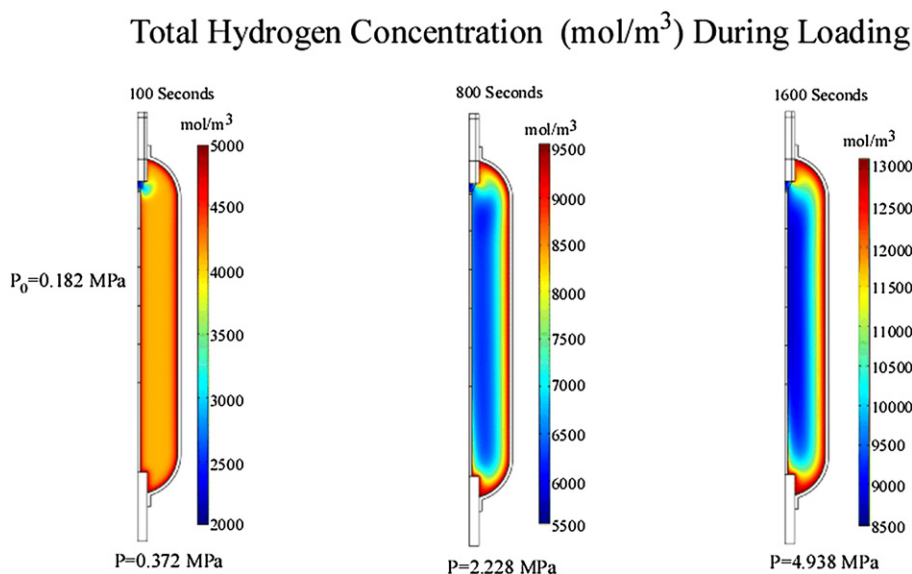


Fig. 5 – Hydrogen concentration profiles during the charging process. In this figure P_0 is the initial pressure and the initial temperature was 80 K.

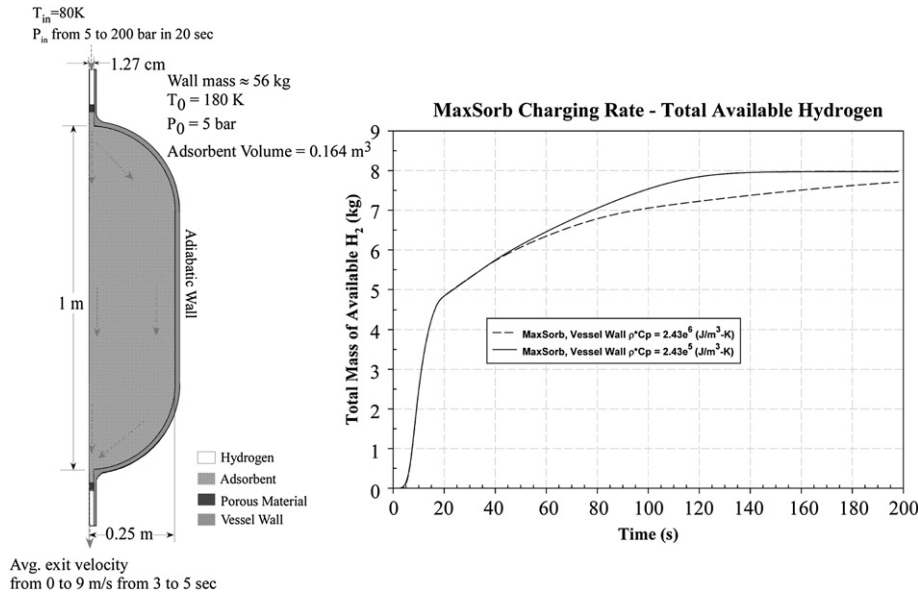


Fig. 6 – The effect of vessel wall heat capacity on charging rates for axial flow-through cooling of MaxSorb. The term ‘available hydrogen’ refers to the amount of hydrogen released upon return to the initial state.

assumed to be at 180 K and 5 bar, which reflects its state upon arrival at the fueling station. To enforce rapid charging of hydrogen the vessel pressure was raised from 5 to 200 bar in 20 s and the temperature of hydrogen entering the vessel was 80 K. The average velocity of hydrogen exiting the vessel, for the purpose of cooling, was allowed to increase from 0 to 9 m/s over a 2 s time interval, starting at 3 s after initiation of the charging transient. The vessel dimensions and geometry are shown in Figs. 6–8, which also show the charging rate of total hydrogen, which includes the adsorbed hydrogen and compressed hydrogen in the void spaces of the adsorbent.

Figs. 6 and 7 show hydrogen charging rates for a vessel cooled by passing hydrogen axially through the adsorbent

bed. Because the vessel wall participates in the transient by way of thermal energy stored at the initial state, the effect of the volumetric heat capacity, (ρC_p) was investigated. Fig. 6 shows the effect of the volumetric heat capacity of the vessel wall on the charging of a MaxSorb™ based vessel. Reducing the volumetric heat capacity of the wall can be seen to markedly affect the rate of hydrogen storage by reducing the initially stored amount of thermal energy that must be removed by convection.

Fig. 7 shows the difference in the rate of hydrogen storage for MaxSorb™ and MOF-5™ based vessels, which are otherwise identical and are charged under the same conditions. From the plot, it can be seen that MOF-5™ charges more rapidly than

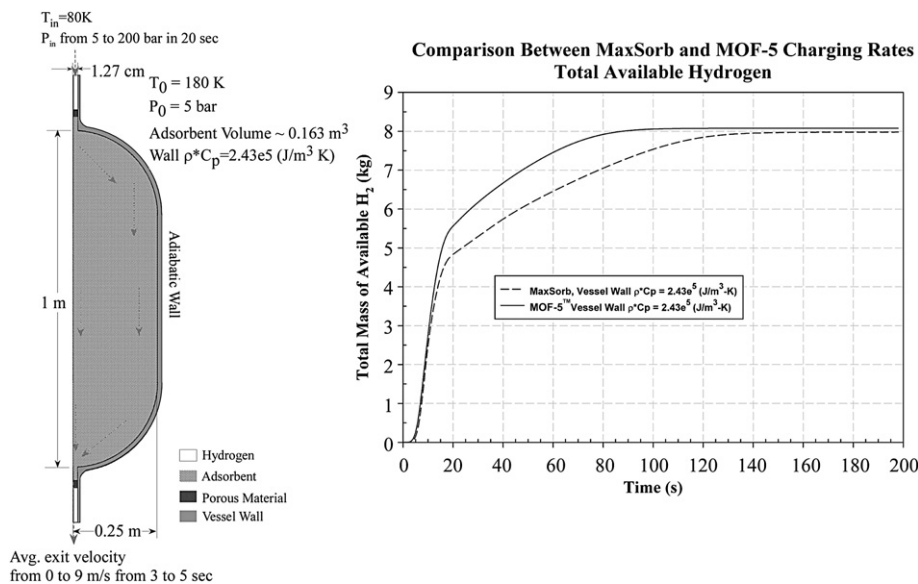


Fig. 7 – Comparison of charging rates for axial flow-through cooling of MaxSorb and MOF-5™.

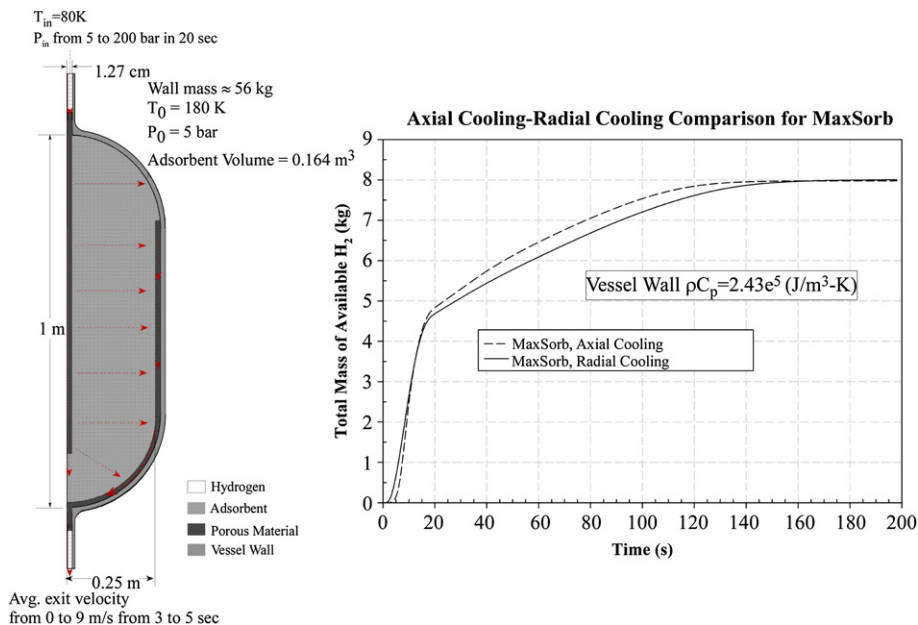


Fig. 8 – Comparison of charging rates for radial and axial flow-through cooling of MaxSorb.

MaxSorb™. The reason for the difference is that the lower volumetric heat capacity, (ρC_p) of MOF-5™, due to its lower bulk density, results in a lower amount of stored thermal energy and, thus, a more rapid reduction in temperature. Because the temperature of the MOF-5™ bed is reduced more quickly, the hydrogen loading rate is increased.

Fig. 8 compares MaxSorb™ charging rates for the axial passage of cooling hydrogen through the adsorbent and for radial passage of hydrogen through the bed. The assumed radial flow configuration is depicted in the schematic in Fig. 8. Here, radial hydrogen flow was achieved by passing hydrogen through a porous rod, having a higher permeability than the bed, along the centerline of the vessel and out through a porous liner, composed of the same material, along the wall of the vessel. For this radial cooling configuration, charging was not quite as rapid as that obtained for axial flow.

4.2.2. Pressure work

As noted in References [12] and [13], pressure work can make significant contribution to the heat released during charging. The rate of heat generation by pressure work is

$$-\epsilon \frac{T}{c} \frac{\partial c}{\partial T} \frac{\partial P}{\partial t} \quad (20)$$

The rate of heat generation due to adsorption is

$$-\frac{\partial}{\partial t} [\rho_{Ads} (\Delta U_a + n_a (u_{H_2O} - u_{H_2}))] \quad (21)$$

Fig. 9 shows the relative contributions of heat generation by pressure work and heat due to adsorption for MOF-5™ and MaxSorb™, in the axial flow-through system shown in Fig. 7. The curves in Fig. 9 show that the contribution of pressure work to the total heat generation can be significant. The relative significance of pressure work depends on: the ratio of gas stored in the adsorbed phase to that in the gas phase, the

adsorbent thermodynamics and the change in pressure. During a transient, the rate of heat transfer will control the local temperature, which, in turn will make the ratio of pressure work to adsorption heat a function of time.

Table 3 gives the total (integral) contribution of pressure work and heat due to adsorption for the MOF-5™ and

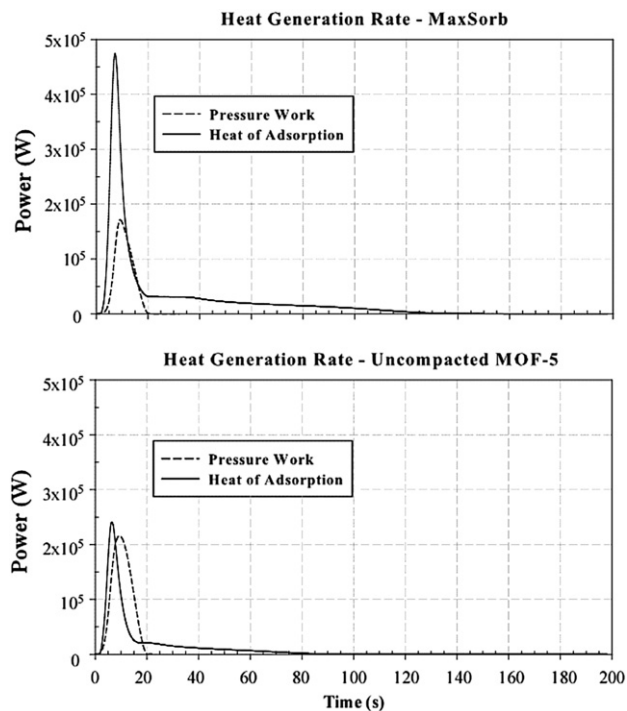


Fig. 9 – Relative contribution of pressure work and heat of adsorption for MaxSorb™ and MOF-5™. System configuration and operating conditions are those of Fig. 7.

Table 3 – Contribution of pressure work and adsorption to heat generation.

	Total Pressure Work (MJ)	Total Adsorption Heat (MJ)	Total Available H ₂ in Adsorbed Volume (kg)	Total Available H ₂ in Gas Volume (kg)
MaxSorb™	1.39	4.81	4.57	3.15
MOF-5™	2.03	2.14	3.40	4.91

MaxSorb™ systems over the charging transient. Also shown in Table 3 are the quantities of available hydrogen stored in the adsorbed volume, V_a , and the gas phase volume.

4.2.3. Exhaust hydrogen for charging with flow-through cooling

The mass of hydrogen exhaust from the vessel and its average temperature for the charging process assumed above, are shown in Table 4. The total mass of available hydrogen for each case in Table 4 is shown in Figs. 6–8. To improve the efficiency of the flow-through cooling process it is desirable to minimize both the mass and average temperature of the exhaust gas, or more precisely to minimize its total enthalpy. Lower total enthalpy better facilitates mixing the exhaust hydrogen with cold hydrogen and using the mixture to initiate cooling and charging of another discharged vessel, which would be at an elevated temperature upon arrival at the fueling station.

4.2.4. Limitations on charging pressure

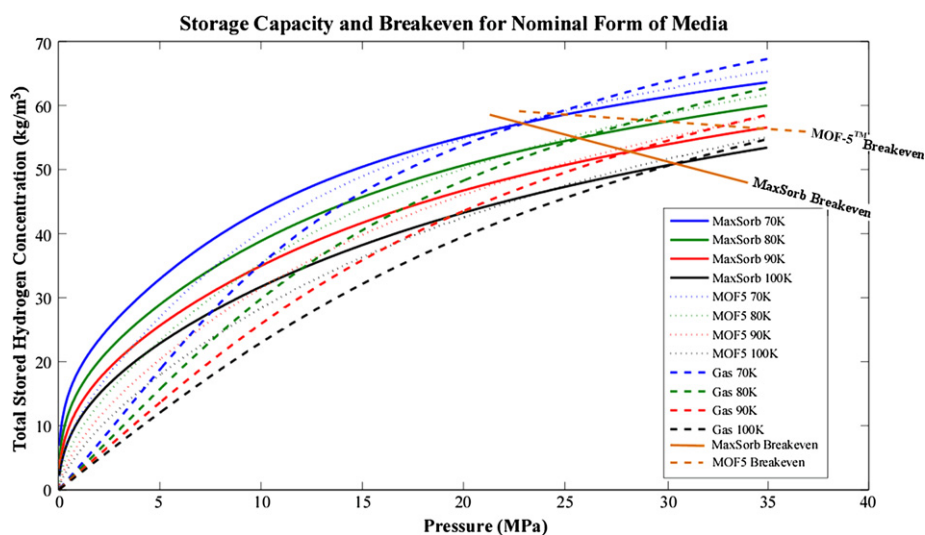
As noted in References [7,23], the mass of hydrogen stored on a volumetric basis by an adsorbent exceeds that stored by compression alone up to a particular pressure. Above this pressure, which depends on temperature, more hydrogen is stored by compression and the advantage of using an adsorbent is lost. The pressure at which storage by pure compression equals that by adsorption is called the breakeven pressure. In hydrogen storage applications the breakeven pressure is a design parameter used to determine whether it is advantageous to use an adsorbent rather than compression alone.

Fig. 10 shows the total mass of stored hydrogen on a volumetric basis for MaxSorb™, MOF-5™ and compression for pressures up to 35 MPa and temperatures of 70, 80, 90 and 100 K. For the adsorbents, the concentration includes adsorbed hydrogen plus compressed hydrogen in the void volume. The compressibility factor from the NIST REFPROP database [6] is used in all calculations for this figure and the adsorbent

Table 4 – Exhaust hydrogen characteristics.

	Charge Time (s)	Mass of Exhaust H ₂ (kg)	Average Exhaust H ₂ Temperature (K)
MaxSorb Low Wall ρ_{C_p}	140	17.9	133.67
MaxSorb Nominal Wall ρ_{C_p}	198 ^a	27.51	120.06
MOF-5™ Low Wall ρ_{C_p}	95	11.61	132.42
MaxSorb Low Wall ρ_{C_p} Radial Cooling	155	19.58	137.49

a Had not reached full capacity.

**Fig. 10 – Storage capacity and breakeven curves for MOF-5™ and MaxSorb.**

storage is based on the Dubinin–Astakhov parameters for each of the adsorbents. For temperatures above 70 K MOF-5™ has higher breakeven pressures than MaxSorb™. The volumetric hydrogen storage capacity for MaxSorb™ exceeds that of MOF-5™ until the pressure approaches the MaxSorb™ breakeven pressure.

5. Summary and conclusions

A general model was developed for adsorbent based hydrogen storage systems. The model was based on systematically derived conservation equations, employed modified Dubinin–Astakhov adsorbent thermodynamics and used real gas properties. The model may readily be applied to a variety of adsorbents, vessel configurations and operating conditions; including charging, discharging and dormancy. System components, including structures and heat transfer devices can be incorporated directly into the model as part of the heat transfer and flow calculations. Calculated parameters include time and spatially dependent pressure, temperature, molar concentrations of hydrogen, the components of gas velocity, gas concentration and/or density. In addition, the model can compute algebraic combinations, integrals and time or spatial derivatives of the above variables. The ability to manipulate dependent variables is essential for evaluation of the performance of storage system designs and for scale-up of prototype tests.

Although the hydrogen adsorption model compared reasonably well with data, there were discrepancies attributed to experimental measurements and material property data. In the comparisons between the model and data, no attempt was made to “tune” input parameters to obtain a better fit. Refinements to the experimental rig will be made to better control inlet hydrogen temperature and measure the surface temperature of the pressure vessel that contains the adsorbent. Specifically, the volume of the Dewar will be increased to ensure that the pressure vessel is always completely surrounded by liquid nitrogen, additional thermocouples will be used to more completely monitor vessel surface temperatures, and the inlet hydrogen temperature will be better controlled through the use of a dedicated heat exchanger. Further, the thermal conductivity of the adsorbent bed will be more accurately measured.

For the flow-through cooling method, the model was used to evaluate:

1. Concept viability
2. Effect of vessel heat capacity and type of adsorbent
3. Effect of radial or axial flow designs
4. Relative importance of pressure work and heat release due to adsorption
5. State of exhaust hydrogen, which is a factor in the efficiency of the charging process.

Calculations for the flow-through system demonstrate the need to control the thermal contact between the adsorbent bed and the vessel wall and/or the heat capacity of the wall. It was found that, under certain conditions, pressure work could be a significant contributor to the total energy released, see

Fig. 9 and Table 3. At higher temperatures less gas is stored by adsorption. Therefore, during the charging process, the fraction of the total energy released due to pressure work increases with increasing temperature.

At temperatures above 70 K the breakeven pressures for MOF-5™ exceed those for MaxSorb™. On a volumetric basis, MaxSorb™ stores more hydrogen than MOF-5™ until the MaxSorb™ breakeven pressure is approached. However, the bulk density of MOF-5™ is half that of MaxSorb™. Hence, the capacity of MOF-5™ is greater on a mass basis. Recent unpublished work suggests that MOF-5™ can be compacted without significant loss of hydrogen storage capacity. If so, it may be possible for its volumetric capacity to be significantly improved.

Acknowledgments

This document was prepared in conjunction with work accomplished under Contract No. DE-AC09-08SR22470 with the U.S. Department of Energy.

Disclaimer

This work was prepared under an agreement with and funded by the U.S. Government. Neither the U. S. Government or its employees, nor any of its contractors, subcontractors or their employees, makes any express or implied: 1. warranty or assumes any legal liability for the accuracy, completeness, or for the use or results of such use of any information, product, or process disclosed; or 2. representation that such use or results of such use would not infringe privately owned rights; or 3. endorsement or recommendation of any specifically identified commercial product, process, or service. Any views and opinions of authors expressed in this work do not necessarily state or reflect those of the United States Government, or its contractors, or subcontractors.

REFERENCES

- [1] Aceves SM, Berry GD, Martinez-Frias J, Espinosa-Loza F. Vehicular storage of hydrogen in insulated pressure vessels. *Int J Hydrogen Energy* 2006;31:2274–83.
- [2] Aceves SM, Espinosa-Loza F, Ledesma-Orozco E, Ross TO, Weisberg AH, Brunner TC, et al. High-density automotive hydrogen storage with cryogenic capable pressure vessels. *Int J Hydrogen Energy* 2010;35:1219–26.
- [3] DOE targets for onboard hydrogen storage systems for light-duty vehicles, rev. 4.0. Available from: http://www1.eere.energy.gov/hydrogenandfuelcells/storage/pdfs/targets_onboard_hydro_storage.pdf [accessed 12.12.11].
- [4] Richard M-A, Bénard P, Chahine R. Gas adsorption process in activated carbon over a wide temperature range above the critical point. Part 1: modified Dubinin–Astakhov model. *Adsorption* 2009;15:43–51.
- [5] Richard M-A, Bénard P, Chahine R. Gas adsorption process in activated carbon over a wide temperature range above the critical point. Part 2: conservation of mass and energy. *Adsorption* 2009;15:53–63.

- [6] Lemmon EW, Huber ML, McLinden MO. NIST Standard Reference Database 23: reference fluid thermodynamic and transport properties-REFPROP, Version 8.0. Gaithersburg: National Institute of Standards and Technology, Standard Reference Data Program; 2007.
- [7] Richard M-A, Cossement D, Chandonia P-A, Chahine R, Mori D, Hirose K. Preliminary evaluation of the performance of an adsorption-based hydrogen storage system. *AIChE J* 2009;11:2985–96.
- [8] Kumar VS, Raghunathan K, Kumar S. A lumped-parameter model for cryo-adsorber hydrogen storage tank. *Int J Hydrogen Energy* 2009;34:5466–75.
- [9] Kumar VS, Kumar S. Generalized model development for a cryo-adsorber and 1-D results for the isobaric refueling period. *Int J Hydrogen Energy* 2010;35:3598–609.
- [10] Bird RB, Stewart WE, Lightfoot EN. *Transport phenomena*. New York, NY: John Wiley & Sons, Inc; 1960.
- [11] Ghosh I, Naskar S, Bandyopadhyay SS. Cryosorption storage of gaseous hydrogen for vehicular application – a conceptual design. *Int J Hydrogen Energy* 2010;35:161–8.
- [12] Hermosilla-Lara G, Momen G, Marty PH, Le Neindre B, Hassouni K. Hydrogen storage by adsorption on activated carbon: investigation of the thermal effects during the charging process. *Int J Hydrogen Energy* 2007;32:1542–53.
- [13] Momen G, Hermosilla G, Michau A, Pons M, Firdaus M, Marty PH, et al. Experimental and numerical investigation of the thermal effects during hydrogen charging in a packed bed storage tank. *Int J Hydrogen Energy* 2009;34:1495–503.
- [14] Zhan L, Li KX, Zhang R. Improvements of the DA equation for application in hydrogen adsorption at supercritical conditions. *J Supercrit Fluids* 2004;28:37–45.
- [15] Paggiaro R, Michl F, Bénard P, Polifke W. Cryo-adsorptive hydrogen storage on activated carbon, II: investigation of the thermal effects during filling at cryogenic temperatures. *Int J Hydrogen Energy* 2010;35:648–59.
- [16] Schütz W, Michl F, Polifke W, Paggiaro R. Storage systems for storing a medium and method for loading a storage system with a storage medium and emptying the same there from. Patent (WO/2005/044454), <http://www.wipo.int/pctdb/en/wo.jsp?wo=2005044454>; 2005.
- [17] Xiao J, Tong I, Deng C, Bénard P, Chahine R. Simulation of heat and mass transfer in activated carbon tank for hydrogen storage. *Int J Hydrogen Energy* 2010;35:8106–16.
- [18] Vasiliev LL, Kanonchik LE. Activated carbon fibres and composites on its base for high performance hydrogen storage system. *Chem Eng Sci* 2010;65:2586–95.
- [19] Pyda M, Bartkowiak M, Wunderlich B. Computation of heat capacities of solids using a general Tarasov equation. *J Thermal Analysis* 2009;52(2):631–56.
- [20] Comsol Multiphysics® 3.5a version 3.5.0.606. Copyright 1998–2008. Comsol AB.
- [21] Critoph RE, Turner L. Heat transfer in granular activated carbon beds in the presence of adsorbable gases. *Int J Heat Mass Trans* 1995;38(9):1577–85.
- [22] Huang BL, Ni Z, Millward A, McGaughey AJH, Uher C, Kaviani M, et al. Thermal conductivity of a metal organic framework (MOF-5): Part II. Measurement. *Int J Heat Mass Trans* 2007;50(3–4):405–11.
- [23] Chahine R, Richard M-A, Cossement D. H₂ storage in nanoporous structures. Presentation, Task 22 IEA HIA Expert Meeting; 6–10 October 2008. Villa Mondragone, Castelli Romani, Italy.